Electron scattering by Fe XXII within the Dirac *R*-matrix approach

S. Ait-Tahar and I. P. Grant
Mathematical Institute, Oxford University, 24-29 St. Giles', Oxford OX1 3LB, United Kingdom

P. H. Norrington
Department of Applied Mathematics and Theoretical Physics, The Queen's University of Belfast, Belfast BT7 1NN, United Kingdom
(Received 18 March 1996; revised manuscript received 6 June 1996)

The Dirac *R*-matrix theory is used to calculate the collision strengths for electron scattering from boronlike iron in the energy range 0–300 Ry. The target model space encompasses 15 fine-structure levels, and all 105 $\Delta n=0$ transitions together with 40 partial waves are included in the calculation. The results are compared with previous semirelativistic *R*-matrix calculations where the relativistic effects are taken into account via some term coupling effects and also with the relativistic distorted wave, which take relativistic effects adequately but do not include effects due to the resonances. We also compare our results with recent Breit-Pauli *R*-matrix calculations where available. We find that there are some important differences between these different calculations. The need to work within a fully relativistic scheme including the resonance effects is stressed. [S1050-2947(96)01310-8]

PACS number(s): 34.80.Kw

I. INTRODUCTION

The study of electron scattering from highly charged ions has been regarded [1–3] as a useful area where theories and approximation schemes are to be tested and physical effects to be investigated. Below the highest threshold, the presence of the resonances in the collision strength is one such effect that needs to be included properly in the calculations, as it affects strongly the effective strengths. Also, relativistic effects have been widely recognized as crucially important, and a serious effort was devoted in the past to incorporating these in the calculations, although mostly in the form of additional corrections or in an approximation scheme. Boronlike ions, being strongly ionized, are very good candidates for the study of both these effects. Most previous work on electron-impact excitation of heavily charged ions involved some kind of limitation. The work of Zhang and Sampson uses the relativistic distorted-wave (RDW) approximation [2]; it is fully relativistic but does not include the resonance and coupling effects on the collision rates. It was shown [1], that when these effects are included, the effective collision rates are enhanced by up to a factor of 2 to 3 in some cases. Calculations based on the close-coupling approximation [1] incorporate these resonance features, but include only limited relativistic effects in an approximation method through the term coupling coefficients (TCC's). This turns out to be a serious limitation, as the collision strengths are substantially affected, especially for some weak but practically important transitions. This was clearly shown in a recent Breit-Pauli (BP) [3] calculation emphasizing the interplay among these different effects.

In order to avoid all of these limitations, one has to work within a full relativistic approach (as pointed out in [1]) while including the resonance effects. One such scheme is the Breit-Pauli-based *R*-matrix approach. Another possibility is to adopt the Dirac equation as the basic equation governing the *R*-matrix calculations [4,5]. A relativistic approach based on the Dirac equation has, besides its elegance, the advantage that all the relativistic effects are included, not in an *ad hoc* way and not only for the eigenenergies but most importantly in the radial wave functions. As is well known, this feature of the Dirac approach makes it the recommended candidate to use for cases involving high-*Z* targets.

Studying B-like ions has also important practical implications. As emphasized in [6], the spectra of these ions are observed from a variety of astrophysical objects, and thus provide valuable density and temperature diagnostics in a wide range of the UV and IR spectra. They are also required in high-temperature plasma research. Accurate atomic data for these ions are therefore much needed for these and other applications.

In order to investigate the limitations of the RDW or TCC approaches in some detail, we look at Fe XXII. For this ion, we consider all transitions, such that $\Delta n=0$, and include all the 15 target levels in our model space. This work also has other motivations: Previous applications of the Dirac based *R*-matrix approach (DARC) for multiply charged ions are very limited and this study builds upon the recent study [7] of electron-impact excitation on H-like ions within this context. It also represents an example of the application of DARC to the study in some detail of the resonance region in electron scattering from ions. It is also useful in relation to the iron project, where one of the continuing objectives is to perform the DARC and BP calculations for these highly ionized targets [3,7]. In Sec. II, we briefly outline the theoretical background to the calculations and present some details of the models for the target states and collision strengths. The results are given in Sec. III: here we discuss these and compare them, when possible, with the TCC and the RDW results drawing particular attention to the regions of energy where disagreement among the various calculations is present. Section IV is devoted to the conclusions.

II. THEORY AND DETAILS OF CALCULATIONS

The theoretical basis for the present calculations has been described in detail elsewhere [4,5,8,9]. It is essentially the

TABLE I. Level indices and designation for the dominant contributing CSF's in Fe XXII.

Level	J^π	Dominant CSF	Weight (%)	LS-coupled
1	$\frac{1}{2}^-$	$2s^2_{1/2}2p_{1/2}$	97.88	$^2P^o_{1/2}$
2	$\frac{3}{2}^-$	$2s^2_{1/2}2p_{3/2}$	97.46	$^2P^o_{3/2}$
3	$\frac{1}{2}^+$	$2s_{1/2}2p^2_{1/2}$	96.11	$^4P_{1/2}$
4	$\frac{3}{2}^+$	$2s_{1/2}2p_{1/2}2p_{3/2}$	99.26	$^4P_{3/2}$
5	$\frac{5}{2}^+$	$2s_{1/2}2p_{1/2}2p_{3/2}$	94.54	$^4P_{5/2}$
6	$\frac{3}{2}^+$	$2s_{1/2}2p_{1/2}2p_{3/2}$	95.12	$^2D_{3/2}$
7	$\frac{5}{2}^+$	$2s_{1/2}2p^2_{3/2}$	94.54	$^2D_{5/2}$
8	$\frac{1}{2}^+$	$2s_{1/2}2p_{1/2}2p_{3/2}$	57.08	$^2P_{1/2}$
9	$\frac{1}{2}^+$	$2s_{1/2}2p^2_{3/2}$	56.39	$^2S_{1/2}$
10	$\frac{3}{2}^+$	$2s_{1/2}2p^2_{3/2}$	95.21	$^2P_{3/2}$
11	$\frac{3}{2}^-$	$2p^2_{1/2}2p_{3/2}$	91.07	$^4S^o_{3/2}$
12	$\frac{3}{2}^-$	$2p_{1/2}2p^2_{3/2}$	82.40	$^2D^o_{3/2}$
13	$\frac{5}{2}^-$	$2p_{1/2}2p^2_{3/2}$	100.00	$^2D^o_{5/2}$
14	$\frac{1}{2}^-$	$2p_{1/2}2p^2_{3/2}$	97.88	$^2P^o_{1/2}$
15	$\frac{3}{2}^-$	$2p^3_{3/2}$	78.33	$^2P^o_{3/2}$

TABLE II. Level energies in Fe XXII in units of kaysers.

Level	J^π	E (MCDF)	E (MCDF+)	E (Kelly)
1	$\frac{1}{2}^-$	0.00	0.00	0.00
2	$\frac{3}{2}^-$	121 890	118 151	118 270
3	$\frac{1}{2}^+$	399 255	398 548	404 550
4	$\frac{3}{2}^+$	456 484	453 721	460 200
5	$\frac{5}{2}^+$	514 131	507 318	513 260
6	$\frac{3}{2}^+$	746 814	742 461	736 520
7	$\frac{5}{2}^+$	770 515	764 231	759 620
8	$\frac{1}{2}^+$	864 137	863 556	853 480
9	$\frac{1}{2}^+$	990 703	986 657	978 220
10	$\frac{3}{2}^+$	1012 078	1005 807	992 290
11	$\frac{3}{2}^-$	1260 042	1254 787	1255 700
12	$\frac{3}{2}^-$	1409 930	1405 895	1396 420
13	$\frac{5}{2}^-$	1444 915	1436 231	1426 880
14	$\frac{1}{2}^-$	1587 022	1582 688	1569 630
15	$\frac{3}{2}^-$	1647 473	1639 408	1627 720

relativistic or Dirac version of the R matrix, as described in, e.g., [5]. As in the nonrelativistic case [10], the configuration space is partitioned into two regions separated by a spherical surface located at a distance $r=a$ (the R-matrix boundary) from the center. This radius is chosen such that the exchange interactions between the projectile electron and the target electrons are negligible beyond this point. In the inner radial region $(r<a)$, the exchange and correlations between the scattered electron and the N-electron target are important, making the $(N+1)$-electron system behave much like a bound state. An approximate wave function of the $(N+1)$-electron system is then constructed and the resulting Hamiltonian diagonalized, yielding the eigenvalues and eigenvectors needed to define the R matrix.

In the outer region, the exchange effects are neglected and the scattered electron wave functions in the different channels are those of an electron moving in the long-range multipole potential of the target. The K matrix is defined by considering the solutions of the asymptotic form of the radial Dirac equations for the scattered electron in this radial region. It is then obtained, for a given energy, by explicitly matching the inner and outer wave functions of the scattered electron at the R-matrix boundary for each channel. From the K matrix, one derives the S matrix from which all the relevant observables, such as the collision strengths and cross sections, are calculated [4,5].

A. Target states

The Oxford code, the GRASP[2] multiconfiguration Dirac-Fock (MCDF) code [11] was used to obtain the wave functions and energies of the B-like Fe target. We are interested in evaluating the collision strengths for transitions between the $n=2$ levels. To this end, all possible configurations, such that $\Delta n=0$, namely $2s^22p,2s2p^2,2p^3$, were included in an average level (AL) calculation, while the $1s^2$ shell was kept full. These jj-coupled CSF's result in a set of 15 levels that are limited to the following symmetry-parity combinations $J^\pi=\frac{1}{2}^\pm,\frac{3}{2}^\pm,\frac{5}{2}^\pm$. These levels are presented in Table I. We also give in that table the dominant CSF's that contribute to these levels and the closest LS-coupled states with which they may be associated. The weights given in Table I are the mixing coefficients squared when transformed from the jj to the LS CSF basis. When transformed to LS-coupled CSF's, all the levels are well designated, except for levels 8 and 9 ($^2P_{1/2}$ and $^2S_{1/2}$), which mix strongly. The MCDF results for the energies are presented in Table II together with the results (MCDF+) obtained when the transverse Breit interaction and QED contributions are included in the calculations. These latter results agree to a reasonable degree (better than 1.5%) with the experimental data taken from the Kelly database. We note here that these results are the same as the ones used in the RDW calculations. These latter were also obtained using the same type of calculation (AL) with the same code [11].

B. Collision strengths

The DARC code was used for this part of the work. This package is similar in structure to the R-matrix package [12] used, for instance, in [1]. All possible 105 transitions among the 15 fine-structure target levels are included in this part of the calculation.

The MCDF+ results were used as input for the threshold energies. The R-matrix boundary was fixed at $r=1.14$ Bohr radii, and the constant b that arises in the boundary condition was set to $b=0$. The radial Dirac equations were solved for 80 continuum angular momenta corresponding to the relativistic quantum number $\kappa=\pm1,\pm2,\ldots,\pm40$, and all partial waves in the range $l=0$–40 were included. Given the range of values of the target angular momentum, this allows for a maximum value of $J=40$ for the total angular momentum of the system.

The Dirac Hamiltonian matrix for the $(N+1)$-electron system in the inner radial region was constructed for each of the J^π combinations $J^\pi=0^\pm,1^\pm,\ldots,40^\pm$, and all possible channels for a given symmetry were incorporated in the calculations. The total number of channels thus generated was 4410, with a dimension of 2240 for the largest Hamiltonian matrix. The use of a finite-size basis set leads naturally to a

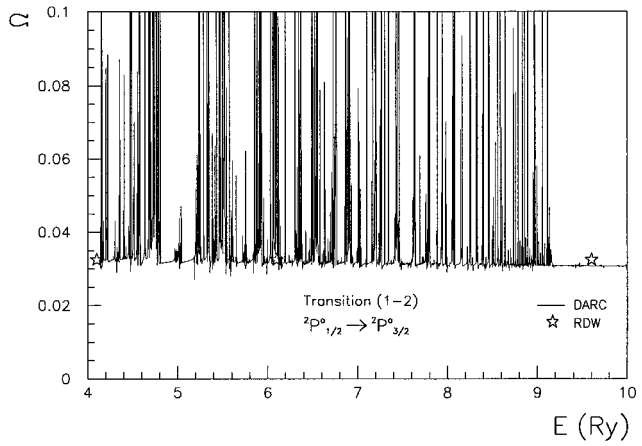

FIG. 1. Collision strength for the weak transition (1–2) in Fe XXII in the resonance-energy region. The solid line indicates the DARC results and the stars give the RDW values.

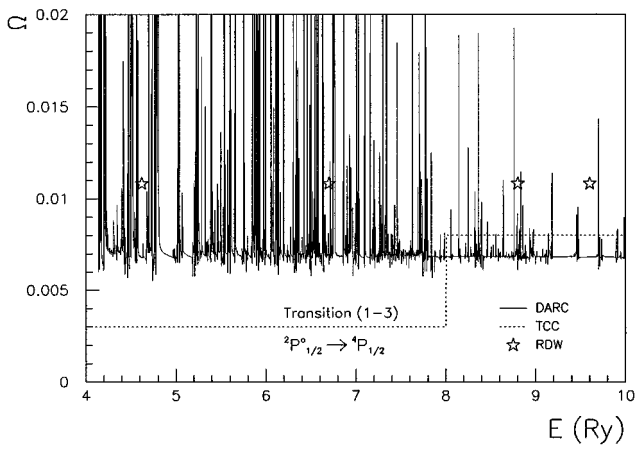

FIG. 2. Collision strength for the spin-forbidden transition (1–3) in Fe XXII in the resonance-energy region. The solid (broken) line indicates the DARC (TCC) results and the stars give the RDW values.

truncation error, and this was corrected for by using the Buttle correction [13].

III. RESULTS AND DISCUSSION

We will compare the present results with those obtained in previous calculations wherever possible. Previous studies of electron-impact excitation on Fe^{21+} include the RDW [2], the TCC [1], and the BP [3] ones, and for this latter work, in the form of a Brief Report, only one transition has been studied for this target ion.

A. Resonance energy region

We will first look at the energy region below the highest threshold; in other words, in the resonance region. This energy region is, as expected, crowded with very narrow and closely spaced resonances. Most of the computational effort goes into mapping out the contour of these resonances and a very-fine-energy mesh is usually required. In the present calculations we use a mesh of 0.005 Ry. Owing to this, previous DARC calculations in this energy region have been limited. It is therefore useful to show that the DARC calculations yield consistent results, not only for the high-energy region, but also for this energy region. In what follows, we will look closely at certain transitions. We will compare separately the transitions that are weak, spin-forbidden, and the optically allowed (dipole) transitions.

First, we consider the weak transition (1–2), i.e., from level 1 to level 2, and this is presented in Fig. 1. The solid line gives the present results while the marker stars indicate the RDW values. The results for the TCC data are not shown in this figure for clarity and they have the same value for the background collision strength. The structure of the resonances is somewhat different for the two calculations, and this is not unexpected, given that different threshold energies are used. The agreement for the background strength is excellent, given that the same value is predicted by the three computations.

The situation for the weak transition (1–11) is somewhat different. Here, the values predicted for the background strength differ substantially. The present value of $\Omega=2.7\times10^{-4}$ is to be compared with the TCC value of $\Omega=1.85\times10^{-4}$ and the RDW result of $\Omega=3.0\times10^{-4}$. The poor agreement between the RDW and TCC results for this transition has also been noted for other ions (Ne VI, Al IX, Ar XIV), and it was slightly surprising to find that our DARC calculations are closer to the RDW result than they are to the TCC one. One would have *a priori* expected to find that the two *R*-matrix-based calculations (TCC and DARC) would have yielded much closer results for the background collision strength in this energy region.

For the intercombination transitions, we will look specifically at the transition from the ground state to the levels 3 and 5. In Fig. 2, we present the collision strength for the (1–3) transition. The DARC collision strength is given by the solid line with a background value of $\Omega=6.85\times10^{-3}$, and the RDW indicated by the stars has a constant value of $\Omega=10.7\times10^{-3}$ for this strength. In this energy region, the strength is dominated by the resonances, and it is difficult to compare the TCC and the DARC fine details, especially as different thresholds are used in the calculations. Thus only the TCC background values are shown in this figure and these are indicated by the dotted line. There is a large jump in these TCC values at the threshold around 8 Ry, and this is related to the onset of the relativistic mixing that is switched on at this energy [1,3]. This situation arises because in the TCC approach the intermediate coupling is used only when the electron energy is greater than the energy of either levels in the transition under consideration. The resonance structure below the excitation threshold is therefore treated nonrelativistically. This is illustrated in Fig. 2, where we see that the TCC background strength jumps from a value of $\Omega=3.0\times10^{-3}$ to $\Omega=8.0\times10^{-3}$, and this is to be compared with the DARC value of $\Omega=6.85\times10^{-3}$, the latter remaining constant throughout the entire energy range.

This problem with the TCC approximation has also been emphasized recently [3] for the case of the intercombination transition (1–5). We also looked at this transition within the Dirac approach in the 4–11-Ry energy range. This energy region is crowded with resonances, and given that the parameters such as the threshold energies used in the calculations are different, it is not necessarily meaningful to attempt a

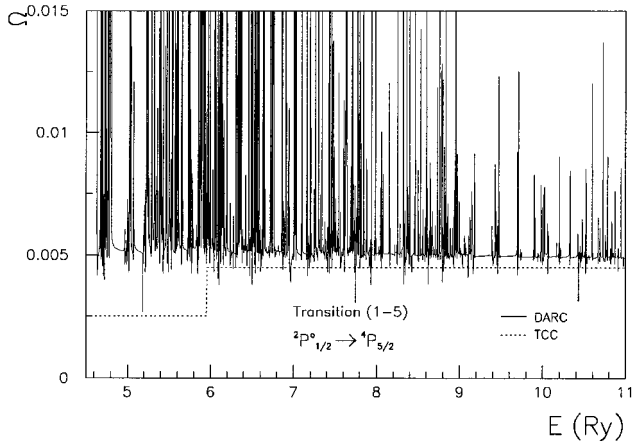

FIG. 3. Collision strength for the spin-forbidden transition (1–5) in Fe XXII in the resonance-energy region. The solid (broken) line indicates the DARC (TCC) results.

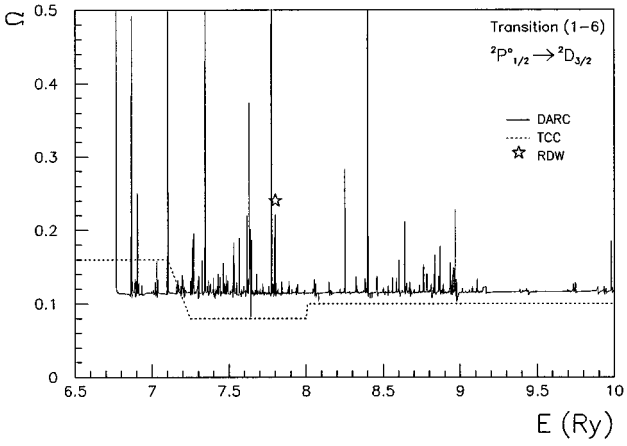

FIG. 4. Collision strength for the dipole transition (1–6) in Fe XXII in the resonance-energy region. The solid (broken) line indicates the DARC (TCC) results and the stars give the RDW values.

close comparison of the details of the collision strengths. However, we find that the overall features for the DARC and BP strengths are similar and the background values are in excellent agreement with Ω (DARC)$=5.0\times10^{-3}$ and Ω (BP)$=5.1\times10^{-3}$ near the higher end of the energy range. The DARC results are presented in Fig. 3 together with the TCC values, and the corresponding BP results may be found in Fig. 1 of Ref. [3]. The TCC background for the transition (1–5) exhibits the same ''jumping'' feature as was observed in the case of transition (1–3) above. The jump occurs at the ^2D threshold around 6 Ry, with the strength being enhanced by a factor of 2 as this threshold is crossed. As reported in [3], this difference in the background value of Ω has important implications: As the total inelastic flux is shared among the coupled channels, the collision strength in the other channels is affected. The Maxwellian averaged rates will reflect these important differences, particularly for these weak (forbidden and intercombination) transitions. Because they are weak, it is necessary to evaluate them accurately owing to the practical relevance they hold for astrophysical and laboratory plasma purposes. Our results confirm the conclusion in [3] that the TCC or other nonrelativistic approximations are not adequate for these ions, especially for the study of these weak transitions. It is thus necessary to work either within the BP approximation or adopt the present approach based on the Dirac R matrix.

Now we turn our attention to the optically allowed transitions in the resonance region. There are four such transitions from the ground state. In contrast to the weak or spin-forbidden transitions, these transitions do not, in general, exhibit a strong resonance effect with relatively fewer resonances superimposed on a smoothly varying background. In Fig. 4, we show the results for the transition (1–6), which is one of the dominant dipole excitations. The structure of the resonances, in the DARC and TCC results, is also reasonably comparable, showing a number of strong resonances and a multitude of smaller ones. In this figure the TCC results for the background strength are indicated by the dotted line and the RDW values are given by the marker stars. The agreement with the TCC calculations is reasonable, with the values for the background being comparable. However, we note that the TCC background shows a small variation with energy, and this feature is absent in the DARC background strength. The RDW value, on the other hand, indicates that the RDW calculations give twice as large a strength as does the R matrix. This is a feature that is found to be characteristic of the RDW calculations at higher energies, and we will discuss this in more detail in what follows. The RDW values for the other dipole transitions from the ground state, namely the (1–8), (1–9), and (1–10) transitions, are also found to be larger than the DARC results.

B. High-energy region

Now we turn our attention to the energy range above the highest threshold. This is the energy region where one would expect the RDW approximation to be particularly good. However, as we will see in the following, we find some discrepancy between the R-matrix results (DARC or TCC) on the one hand and the RDW calculations on the other for the dipole transitions. These transitions are, of course, the strongest ones among all the possible transitions being connected to the ground state by the electric dipole operator. In Fig. 5, the collision strengths of the optically allowed transitions from the ground state to the levels in our model space are shown in the energy range 20–250 Ry. These are the DARC results and compare reasonably well with the TCC calculations. This is not the situation with regard to the RDW results, which are consistently higher over most of the energy range. The RDW values are shown as stars (joined by straight lines for convenience). One would first think that this may be due to a redistribution of strengths among all these inelastic channels, but a close inspection reveals that it is not the case.

Indeed, as Fig. 5 indicates, this discrepancy persists for all these dipole excitations, and the total dipole strength reflects this situation. Furthermore, we find that for all dipole transitions among the different levels (and there are 29 such transitions in all) the same remarks can be made. As an example of transitions from other than the ground state, we present in Fig. 6 the collision strength from level 5 to level 11 in the energy range 40–150 Ry. Although the DARC and RDW values agree below 80 Ry, the RDW gives an increasingly higher estimate for the strength as the energy is increased. As

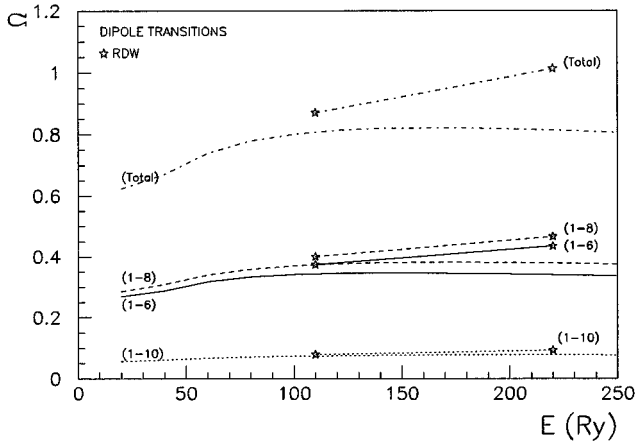

FIG. 5. Dipole collision strength for the transitions (1–6), (1–8), (1–10), and the total dipole strength in Fe XXII in the high-energy region. The curved lines are the DARC results and the RDW values are given by the stars (which are joined by straight lines for convenience).

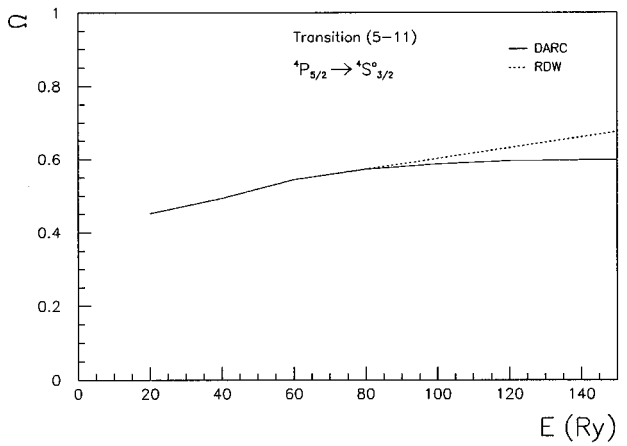

FIG. 6. Collision strength for the dipole transition (5–11) in Fe XXII in the high-energy region. The solid (broken) line indicates the DARC (RDW) results.

reported in [1], the same situation is noticed when comparing the RDW and TCC results, with the RDW values being larger than the TCC ones.

Thus it seems that, for these transitions above the highest threshold energy, the RDW results for the collision strengths are larger than either the TCC or DARC results. This situation needs investigating. The existing discrepancy amounts to about 10% at around 100 Ry. One possible source that may contribute to this discrepancy between the RDW and the R-matrix calculation is related to the number of partial waves actually included in the calculation. Whereas in the present work, we have included explicitly all partial waves up to ($l=40$), in the RDW work only 28 and 32 partial waves are included at around 100 and 200 Ry, respectively, and the Coulomb-Bethe approximation (CBA) is then used to incorporate the effects from the higher partial waves. The TCC calculations where the CBA is also used nevertheless gives estimates that are lower than the RDW ones. It is thus possible that this latter contribution (CB) in the RDW could be too large and thus lead to an overestimation of the total collision strength for each transition. In order to ascertain this, one needs to compare the CB contribution in both the TCC and the RDW calculations, and it would be helpful if these contributions were given explicitly in the future.

However, other sources for this discrepancy remain possible. Our results are 100% converged for the weak transitions, and given the large number of partial waves included explicitly, we estimate that the dipole strengths are nearly converged. A simple test, although not totally justified, based on the strength evolving as a geometric progression, also indicates that convergence is achieved in the present calculations. It is clear that to settle the matter definitively the next step is to include even higher partial waves within a procedure such as the CBA for fine-structure transitions. This needs to be looked at in the future. Nevertheless, there remains the possibility that for these strong transitions, the RDW is yielding excess strength. If this is the case, then it may arise as a result of a choice of model-dependent parameters or in a more serious way could reflect some basic limitation to the RDW. Distorted-wave theories are essentially less ambitious than extensive coupled-channel approaches (e.g., R-matrix), and they are known to be poor approximations in instances where channel coupling is particularly strong. The preceding comments should nevertheless be put into perspective: The discrepancies between the DARC and the RDW results in this energy region are not unexpected or unreasonable. Discrepancies of the order found here (10–20 % or even higher) have been reported when comparing R-matrix-based calculations with distorted-wave ones (for instance, see [5,14]) and also between different distorted-wave calculations (e.g., see compilations for various ions in the same reference and volume as [14]).

Still considering these dipole transitions, there are also some small discrepancies between the two R-matrix calculations in an intermediate-energy region just above the highest threshold. At around 20 Ry, the DARC and RDW results are in very good agreement, and the TCC values are the odd ones out. For the transition (1–6) shown in Fig. 5, the DARC and RDW both give a value of $\Omega=0.27$ at 20 Ry, whereas the TCC value ($\Omega=0.17$) is substantially lower. At the same energy for the transition (5–11) in Fig. 6, the RDW and DARC estimates are the same ($\Omega=0.45$), while the TCC value ($\Omega=0.37$) is lower.

Looking at the weak transitions in the high-energy range, we find that overall the agreement between the RDW, TCC, and the DARC is reasonably good. In Figs. 7 and 8, we present the results for the transitions (1–2) and (1–11), respectively. For the first transition, the agreement among the three calculations is very good over the entire energy range. For the transition (1–11), we find the same situation, except at the low end of the range around 20 Ry where the TCC value ($\Omega=1.8\times10^{-4}$) is appreciably smaller than the RDW value ($\Omega=2.8\times10^{-4}$) or the DARC one ($\Omega=2.6\times10^{-4}$).

IV. CONCLUSIONS

We have carried out a Dirac R-matrix calculation of the electron excitation of the boronlike Fe ion, including all possible $\Delta n=0$ transitions. We looked in some detail at the entire energy region from the lowest threshold to 300 Ry. We find that in the resonance-energy region, the RDW is limited in that it does not take into account the resonance

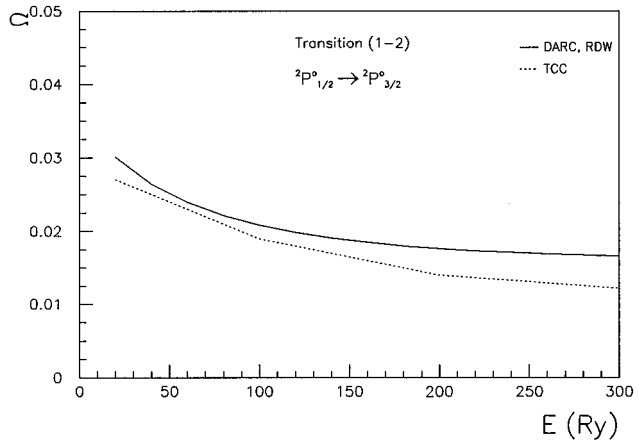

FIG. 7. Collision strength for the weak transition (1–2) in Fe XXII in the high-energy region. The solid (broken) line indicates the DARC (TCC) results. The RDW line nearly merges with the DARC one and is not shown here.

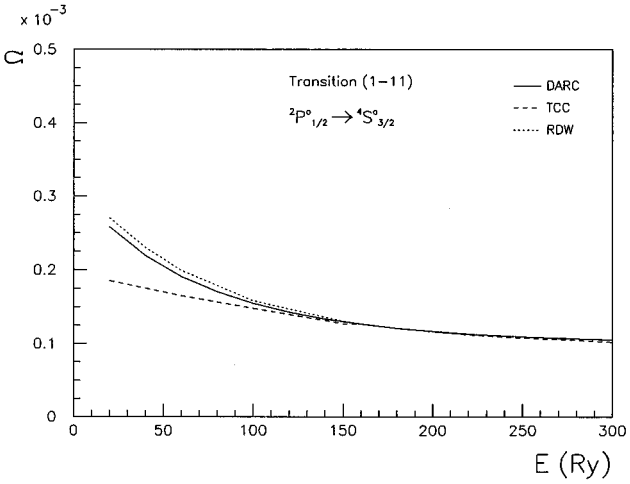

FIG. 8. Collision strength for the weak transition (1–11) in Fe XXII in the high-energy region. The solid line indicates the DARC results and the dotted (dashed) line gives the RDW (TCC) values.

effects, while the TCC has a serious limitation in that the relativistic effects are taken into account only in an approximate way, leading to large jumps in the background strengths. In the intermediate-energy region around 20 Ry, the TCC results seem to give lower estimates for the strength than the DARC or RDW values. In the high-energy region, we find that the RDW estimates are much larger than either the TCC or the DARC ones for the case of dipole transitions. We argued that this effect is not due to some redistribution of flux among the different channels.

This work extends the BP study made in [3] for the transition (1–5) in Fe^{21+} to other transitions, and reinforces the conclusions reached there that for multiply charged target ions both the resonance and relativistic effects play an important role and need to be properly taken into account. It would be interesting to compare the BP and the DARC results in much more detail for a number of transitions in the future. This would require that the calculations are done using similar ingredients (threshold energies) in order to make such a comparison more meaningful.

Besides this, our motivation is also geared towards showing that the DARC-type calculations are practically feasible at all energies, including the resonance-energy region. This work points out to the need to work within a consistent framework where the above effects are included. These relativistic effects can be taken into account adequately within a BP approach for low-Z targets, but as one goes to higher Z values, it becomes necessary to include the full relativistic effects that will be reflected not solely in the energies but most importantly in the electronic wave functions. Given that most of the computational effort is needed in the mapping out of the resonance region, it makes sense to use a fully relativistic approach to the study of electron elastic and inelastic excitation processes and to use the DARC approach right throughout the range of Z values ($26 \leqslant Z \leqslant 92$) and not restrict its use to the high-Z region.

ACKNOWLEDGMENT

An EPSRC research grant in support of S.A. is gratefully acknowledged.

[1] H. L. Zhang and A. K. Pradhan, Phys. Rev. A **50**, 3105 (1994).
[2] H. L. Zhang and D. H. Sampson, At. Data Nucl. Data Tables **56**, 41 (1994).
[3] H. L. Zhang and A. K. Pradhan, J. Phys. B **28**, L285 (1995).
[4] J. J. Chang, J. Phys. B **8**, 2327; **10**, 3335 (1975).
[5] P. H. Norrington and I. P. Grant, J. Phys. B **20**, 4869 (1987).
[6] H. L. Zhang, M. Graziani, and A. K. Pradhan, Astron. Astrophys. **283**, 319 (1994).
[7] R. Kisielius, K. A. Berrington, and P. H. Norrington, J. Phys. B **28**, 2459 (1995).
[8] W. P. Wijesundera, F. A. Parpia, I. P. Grant, and P. H. Norrington, J. Phys. B **24**, 1803 (1991).
[9] W. P. Wijesundera, I. P. Grant, P. H. Norrington, and F. A. Parpia, J. Phys. B **24**, 1017 (1991).
[10] P. G. Burke, A. Hibbert, and W. D. Robb, J. Phys. B **4**, 153 (1971).
[11] K. G. Dyall, I. P. Grant, C. T. Johnson, F. A. Parpia, and E. P. Plummer, Comput. Phys. Commun. **55**, 425 (1989).
[12] K. A. Berrington, P. G. Burke, K. Butler, M. J. Seaton, K. T. Taylor, and Yan Yu, J. Phys. B **20**, 6379 (1987).
[13] P. J. A. Buttle, Phys. Rev. **160**, 719 (1967).
[14] D. H. Sampson, H. L. Zhang, and C. J. Fontes, At. Data Nucl. Data Tables **57**, 97 (1994).